Mon. Not. R. Astron. Soc. **345,** 153–160 (2003)

The termination shock in a striped pulsar wind

Y. E. Lyubarsky★
Physics Department, Ben-Gurion University, PO Box 653, Beer-Sheva 84105, Israel

Accepted 2003 June 17. Received 2003 May 26; in original form 2003 March 4

ABSTRACT

The origin of radio emission from plerions is considered. Recent observations suggest that radio-emitting electrons are presently accelerated rather than having been injected at early stages of the plerion evolution. The observed flat spectra without a low-frequency cut-off imply an acceleration mechanism that raises the average particle energy by orders of magnitude but leaves most of the particles at an energy of less than approximately a few hundred MeV. It is suggested that annihilation of the alternating magnetic field at the pulsar wind termination shock provides the necessary mechanism. Toroidal stripes of opposite magnetic polarity are formed in the wind emanating from an obliquely rotating pulsar magnetosphere (the striped wind). At the termination shock, the flow compresses and the magnetic field annihilates by driven reconnection. Jump conditions are obtained for the shock in a striped wind. It is shown that the post-shock magnetohydrodynamic parameters of the flow are the same as if the energy of the alternating field had already been converted into plasma energy upstream of the shock. Therefore, the available estimates of the ratio of the Poynting flux to the matter energy flux, σ, should be attributed not to the total upstream Poynting flux but only to that associated with the average magnetic field. A simple model for the particle acceleration in the shocked striped wind is presented.

Key words: acceleration of particles – magnetic fields – MHD – shock waves – pulsars: general – supernova remnants.

1 INTRODUCTION

Most of the pulsar spin-down power is carried away by a relativistic, magnetized wind. The pulsar wind injects this energy into the surrounding nebula in the form of relativistic electron–positron pairs and magnetic fields, therefore such nebulae, or plerions, emit synchrotron radiation from the radio to the gamma-ray band. The most famous and well-studied example of the plerion is the Crab Nebula; the spectrum of this source is measured from approximately 10 MHz to dozens of TeV. According to magnetohydrodynamic (MHD) models (Rees & Gunn 1974; Kennel & Coroniti 1984; Emmering & Chevalier 1987; Begelman & Li 1992), the pulsar wind terminates in a standing shock at a radius defined by the condition that the confining pressure balances the momentum flux of the wind. In the case of the Crab, the shock radius was estimated to be 3×10^{17} cm in excellent agreement with observations; according to results from *Chandra* (Weisskopf et al. 2000), the radius of the shock in the equatorial plane is 4×10^{17} cm. The observed brightness and the spectral index distributions are generally consistent with the assumption that the relativistic particles are accelerated at the termination shock and then fill in the nebula, spending the acquired energy on synchrotron emission and $p\,\mathrm{d}V$ work.

The generic observational feature of plerions is a flat radio spectrum; the spectral flux may be presented as a power-law function of the frequency, $\mathcal{F}_\nu \propto \nu^{-\alpha}$, with spectral index $\alpha = 0$–0.3. At high frequencies the spectrum steepens and the typical spectral slope in the X-ray band is $\alpha \gtrsim 1$. The overall spectrum of the Crab may be described as a broken power law with spectral breaks around 10^{13} Hz, a few $\times 10^{15}$ Hz and around 100 keV. The synchrotron lifetime of the radio-emitting electrons (and positrons – below by electrons I mean both electrons and positrons) significantly exceeds the plerion age, therefore one cannot exclude a priori the possibility that they were injected at a very early stage of the plerion evolution (Kennel & Coroniti 1984; Atoyan 1999). In this case the overall spectrum depends on the history of the nebula. However, the spectral break at 10^{13} Hz may be simply accounted for by the synchrotron burn-off effect, assuming that particles emitting from the radio to the optical bands are injected more or less homogeneously in time with a single power-law energy distribution. This view is strongly supported by Gallant & Tuffs (1999, 2002), who found that the infrared spectral index in the central parts of the Crab is close to that in the radio band, and gradually steepens outwards. Recent observations of wisps in the radio band (Bietenholtz & Kronberg 1992; Bietenholtz, Frail & Hester 2001) suggest unambiguously that the radio-emitting

★E-mail: lyub@bgumail.bgu.ac.il

electrons are accelerated now in the same region as those responsible for the optical to X-ray emission.

If the radio-emitting electrons have been injected into the Crab Nebula up to the present time, the injection rate of electrons should be approximately 10^{40}–10^{41} s^{-1}. It is interesting that the observed pulsed optical emission from the Crab pulsar suggests that approximately the same number of electrons are ejected from the pulsar magnetosphere (Shklovsky 1970) so the pulsar does supply the necessary number of particles. The observed spectral slope in the radio band, $\alpha = 0.26$, implies an energy distribution for the injected electrons of the form $N(E) \propto E^{-3/2}$. In this case, most of the particles find themselves at the low-energy end of the distribution, whereas particles at the upper end of the distribution dominate the energy density of the plasma. Taking into account the fact that no sign of a low-frequency cut-off is observed in the Crab spectrum down to approximately 10 MHz, whereas the high-frequency break lies in the ultraviolet band (recall that the break at approximately 10^{13} Hz is attributed to synchrotron cooling but not to the injected energy distribution), one concludes that the above distribution extends from $E_{\rm min} \lesssim 100$ MeV to $E_{\rm max} \sim 10^6$ MeV. At $E > E_{\rm max}$ the distribution becomes steeper; the spectral slope in the X-ray band, $\alpha = 1.1$, corresponds, accounting for the synchrotron burn-off effect, to $N(E) \propto E^{-2.2}$. The distribution further steepens at $E \sim 10^9$ MeV as it follows from the gamma-ray spectrum of the Crab Nebula. Thus the injected electrons have a very wide energy distribution, their number density being dominated by low-energy electrons, whereas the plasma energy density is dominated by TeV electrons.

The above considerations place severe limits on the pulsar wind parameters and possible mechanisms for particle acceleration at the termination shock. According to the widespread view, the pulsars emit Poynting-dominated winds, however, the electromagnetic energy is efficiently transferred to the plasma flow such that the magnetization parameter σ, defined as the ratio of the Poynting flux to the kinetic energy flux, is already very small when the flow enters the termination shock. The mechanisms of such an energy transfer still remain unclear (the so-called σ-problem) however, the dynamics of the flow in the Crab Nebula suggests that the magnetic pressure is small just beyond the termination shock, which implies that the Poynting flux just upstream of the shock is very small (Rees & Gunn 1974; Kundt & Krotscheck 1980; Kennel & Coroniti 1984; Emmering & Chevalier 1987; Begelman & Li 1992). In this case it is the kinetic energy of the upstream flow that converts into the energy of accelerated particles when the plasma flow is randomized at the shock. Then the characteristic downstream 'temperature' is approximately the upstream particle kinetic energy, $T \sim mc^2\Gamma_{\rm w}$, so the average particle energy does not vary considerably across the shock. A high-energy tail may be formed in the particle energy distribution (the particle acceleration at the relativistic shocks is considered by Hoshino et al. 1992; Gallant & Arons 1994; Bednarz & Ostrowski 1998; Gallant & Achterberg 1999; Kirk et al. 2000; Achterberg et al. 2001), however, this tail merges, at its low-energy end, with the quasi-thermal distribution at $E \sim T \sim mc^2\Gamma_{\rm w}$. Therefore, if the pulsar spin-down power, $L_{\rm sd}$, is converted into kinetic energy of the wind, the available upper limit on the low-frequency break in the Crab spectrum suggests that the wind Lorentz factor, $\Gamma_{\rm w}$, does not exceed a few hundred.

On the other hand, the observed flat spectrum may be formed only if the energy per electron in the wind is much larger than $m_{\rm e}c^2\Gamma_{\rm w}$. Gallant et al. (2002), modifying the original idea of Hoshino et al. (1992) and Gallant & Arons (1994), suggested that the wind is loaded by ions; in this case the radio-emitting electrons are accelerated by resonant absorption of ion cyclotron waves collectively emitted at the shock front. The necessary ion injection rate, $\sim L_{\rm sd}/(m_{\rm p}c^2\Gamma_{\rm w}) \sim 10^{39}$ s^{-1}, vastly exceeds the fiducial Goldreich–Julian elementary charge loss rate, $\sim 3 \times 10^{34}$ s^{-1}. Although one cannot exclude by observation the possibility that pulsars emit the required number of ions, the available pulsar models do not assume an ion outflow with a rate exceeding the Goldreich–Julian charge loss rate (Cheng & Ruderman 1980; Arons 1983).

Here I consider an alternative possibility, which does not imply a radical modification of the basic pulsar model. In the equatorial belt of the wind from an obliquely rotating pulsar magnetosphere, the sign of the magnetic field alternates with the pulsar period, forming stripes of opposite magnetic polarity (Michel 1971, 1982; Coroniti 1990; Bogovalov 1999). Observations of X-ray tori around pulsars (Weisskopf et al. 2000; Gaensler, Pivovaroff & Garmire 2001; Helfand, Gotthelf & Halpern 2001; Pavlov et al. 2001; Gaensler et al. 2002; Lu et al. 2002) suggest that it is in the equatorial belt where most of the wind energy is transported; theoretical models (e.g. Bogovalov's 1999, solution for the oblique split monopole magnetosphere) support this conclusion. Therefore, the fate of the striped wind is of special interest. In the striped wind, the Poynting flux converts into the particle energy flux when the oppositely directed magnetic fields annihilate (Coroniti 1990; Lyubarsky & Kirk 2001, henceforth LK; Lyutikov 2002; Kirk & Skjæraasen 2003). Until now this dissipation mechanism was considered only in the unshocked wind. It was found that the flow acceleration in the course of the energy release dilates the dissipation time-scale so that the wind may enter the termination shock before the alternating field annihilates completely. In this case driven annihilation of the magnetic field at the shock may provide the energy necessary to form the flat particle distribution. On the other hand, the formed distribution may extend down to low enough energy because the kinetic energy of the flow in the striped wind is lower than the total energy. The aim of this research is to consider properties of the termination shock in the striped wind.

It will be shown that the alternating field completely annihilates at the shock so that the downstream parameters of the flow are the same as if the field has already annihilated upstream of the shock. Therefore, the available limits on the upstream magnetization parameter, σ, should be attributed not to the total Poynting flux but to the Poynting flux associated with the averaged magnetic field (see also Rees & Gunn 1974; Kundt & Krotscheck 1980). The upstream flow may be Poynting-dominated provided most of the Poynting flux is transferred by an alternating magnetic field. On the other hand, driven reconnection of the magnetic field within the shock radically alters the particle acceleration process. It follows from both analytical and numerical studies that particles are readily accelerated in the course of the magnetic field reconnection to form an energy distribution with the power-law index $\beta \sim 1$ (Romanova & Lovelace 1992; Zenitani & Hoshino 2001; Larrabee, Lovelace & Romanova 2003). Electrons with such a distribution emit synchrotron radiation with a flat spectrum therefore Romanova & Lovelace (1992) and Birk, Crusius-Wätzel & Lesch (2001) suggested that reconnection plays a crucial role in flat spectrum extragalactic radio sources. One can naturally assume that radio emission of plerions is generated by electrons accelerated in the course of reconnection of the alternating magnetic field at the pulsar wind termination shock. Then the steeper high-energy spectrum may be attributed to the Fermi acceleration of particles preaccelerated in the reconnection process. A simple model for particle acceleration in the shocked striped wind is presented here. It will be shown that the minimal energy of the power-law energy distribution may be low in this case, even less then the upstream kinetic energy, whereas the energy density of the

plasma will be dominated by high-energy electrons in agreement with the observed spectra of plerions.

The article is organized as follows. Jump conditions for a shock in the striped wind are obtained in Section 2. Making use of these jump conditions, in Section 3 I demonstrate that the alternating magnetic field dissipates completely at the pulsar wind termination shock. In Section 4 I discuss particle acceleration by driven reconnection. Particle acceleration at the shock in the striped wind is analysed in Section 5. The results obtained are summarized in Section 6.

2 JUMP CONDITIONS FOR THE SHOCK IN A STRIPED WIND

Let us find jump conditions for a shock in a flow with an alternating magnetic field (see also Levinson & van Putten 1997, who considered the relativistic MHD shock with dissipation). The plasma upstream of the shock is assumed to be cold everywhere with the exception of narrow current sheets separating stripes of opposite magnetic polarity. The pressure balance implies that the magnetic field strength in adjacent stripes differs only in sign, but not in absolute value; on the other hand, the width of stripes with opposite polarity may not be the same so that the average magnetic field may be non-zero (Fig. 1). One generally finds jump conditions from the conservation laws and some prescription for the magnetic flux passing the shock. In the standard MHD shock, the magnetic flux is conserved; in the case under consideration one should choose a more general prescription to take into account possible annihilation of the magnetic field at the shock.

Outside the shock, the magnetic field is frozen into the plasma, $\boldsymbol{E} + (1/c)\,\boldsymbol{v} \times \boldsymbol{B} = 0$. In the case of interest the magnetic field lies in the plane of the shock. In the frame where the flow velocity is perpendicular to the shock plane $E = (v/c)B$. Then the Faraday law may be written as

$$\frac{\partial B}{\partial t} + \frac{1}{c}\frac{\partial}{\partial x} vB = 0.$$

Together with the continuity equation

$$\frac{\partial}{\partial t}\Gamma n + \frac{\partial}{\partial x}\Gamma n v = 0,$$

this implies

$$\frac{B}{n\Gamma} = b, \tag{1}$$

where Γ and n are the Lorentz factor and the proper plasma density, respectively, and b is a constant for each fluid element. The energy and momentum fluxes are

$$S = w\Gamma^2 v + \frac{EB}{4\pi}c,$$

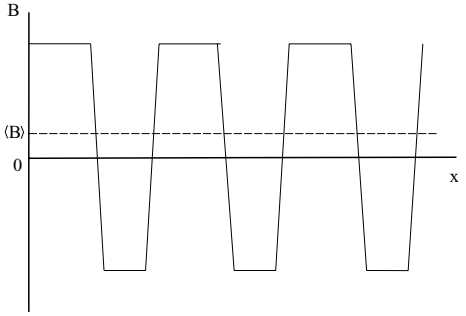

Figure 1. The magnetic field in the striped wind. The average field is shown as a dashed line.

$$F = w\Gamma^2(v/c)^2 + p + \frac{E^2 + B^2}{8\pi},$$

where p and w are the gas pressure and specific enthalpy, respectively. Taking into account the above considerations, one can write

$$S = \mathcal{W} v \Gamma^2, \qquad F = \mathcal{W}\Gamma^2(v/c)^2 + \mathcal{P}, \tag{2}$$

where the effective pressure and enthalpy are

$$\mathcal{P} = p + \frac{b^2 n^2}{8\pi}, \qquad \mathcal{W} = w + \frac{b^2 n^2}{4\pi}, \tag{3}$$

so the flow may be described by the hydrodynamical equations.

In the standard MHD theory, the magnetic flux is conserved and the flow is considered to be homogeneous both upstream and downstream of the shock so that b is a global constant. In our case b is an alternating function of the Lagrangian coordinate, however, only b^2 enters the conservation laws therefore the only essential difference from the standard MHD theory is that the modulus b may decrease in the shock because of the field annihilation. Let us introduce a parameter

$$\eta = \frac{b_2^2}{b_1^2} \tag{4}$$

to measure the decrease of magnetic flux across the shock. The indices 1 and 2 are referred to quantities upstream and downstream of the shock, correspondingly.

One can express the downstream parameters via the upstream ones by making use of the conservation of the particle, energy and momentum fluxes across the shock. Radiation losses may be safely neglected at the shock width scale. In the striped wind, one should take the fluxes averaged over the wave period. Let us assume, for the sake of simplicity, that the current sheets between the stripes are so narrow that one can neglect the contribution of the plasma within the sheets into the conserving fluxes. Outside the sheets, the magnetic field and plasma density are constant across a stripe and the adjacent stripes differ only in the sign of the magnetic field and the width. Taking into account that the energy and momentum fluxes are proportional to the magnetic field squared, one can write the conservation laws such as in the case of homogeneous magnetic field:

$$v_1\Gamma_1 n_1 = v_2\Gamma_2 n_2, \tag{5}$$

$$\mathcal{W}_1 v_1 \Gamma_1^2 = \mathcal{W}_2 v_2 \Gamma_2^2, \tag{6}$$

$$\mathcal{W}_1\Gamma_1^2(v_1/c)^2 + \mathcal{P}_1 = \mathcal{W}_2\Gamma_2^2(v_2/c)^2 + \mathcal{P}_2. \tag{7}$$

The only formal difference from the case of the standard MHD shock is in the additional parameter $\eta \leqslant 1$ (in the standard shock $\eta = 1$).

One can resolve the above equations as follows. The plasma downstream of the shock is relativistically hot, $w_2 = 4p_2$, therefore one can easily eliminate w and p from equation (3) and express $\mathcal{P}_2$ via $\mathcal{W}_2$ and n_2. Substituting the relation obtained into equation (7), one then eliminates $\mathcal{W}_2$, making use of equation (6) and eliminates n_2, making use of equation (5). Taking into account that the plasma upstream of the shock is cold, $p_1 = 0$ and $w_1 = nm_e c^2$, one obtains the resulting equation for the downstream velocity in the form

$$\left(1 + \frac{1}{\sigma}\right)\left(v_1 - v_2 - \frac{c^2}{4v_2\Gamma_2^2}\right)\frac{\Gamma_1^2 v_1}{c^2} + \frac{1}{2} = \frac{\eta}{4}\frac{v_1^2\Gamma_1^2}{v_2^2\Gamma_2^2} - \frac{v_1\Gamma_1}{4\sigma v_2\Gamma_2}, \tag{8}$$

where

$$\sigma = \frac{b_1^2 n_1}{4\pi m_e c^2} \tag{9}$$

is the magnetization parameter. This equation is exact. In the case where $\Gamma_1^2 \gg \mathrm{Max}\ (\sigma, 1)$ one can take $v_1 = c$. Then equation (8) reduces to

$$(3v_2 - c)\left(1 + \frac{1}{\sigma}\right) = \frac{\eta c}{v_2}(c + v_2).$$

Now the downstream parameters may be found explicitly:

$$v_2 = \frac{c}{6}(1 + \chi + \sqrt{1 + 14\chi + \chi^2}), \tag{10}$$

$$n_2 = n_1\Gamma_1 \frac{\sqrt{2[17 - 8\chi - \chi^2 - (1+\chi)\sqrt{1 + 14\chi + \chi^2}]}}{1 + \chi + \sqrt{1 + 14\chi + \chi^2}}, \tag{11}$$

$$\frac{T_2}{m_e c^2} = \frac{\Gamma_1(1+\sigma)}{12\sqrt{2}}\sqrt{17 - 8\chi - \chi^2 - (1+\chi)\sqrt{1 + 14\chi + \chi^2}} \times\left(1 - \frac{6\chi}{1 + \chi + \sqrt{1 + 14\chi + \chi^2}}\right), \tag{12}$$

where

$$\chi = \frac{\eta\sigma}{1+\sigma}. \tag{13}$$

At $\eta = 1$ one recovers the downstream parameters for the relativistic MHD shock in the homogeneous medium (Kennel & Coroniti 1984; Appl & Camenzind 1988). In this case the quantity χ is the ratio of the upstream Poynting flux to the total energy flux. In a striped wind, χ is determined by the Poynting flux corresponding to the magnetic flux passing the shock. It will be shown in the next section that the alternating magnetic field annihilates completely at the pulsar wind termination shock; then χ is simply the ratio of the Poynting flux associated with the average magnetic field, $\langle B_1\rangle^2 v/4\pi$, to the total energy flux. At the equator of the flow the average field is zero, $\alpha = 0$, therefore one obtains $v_2 = c/3$, such as at the non-magnetized relativistic shock. When the average magnetic flux is large, $\sigma \gg 1$, $\eta \to 1$, the downstream flow is relativistic with the Lorentz factor

$$\Gamma_2 = \sqrt{\frac{\sigma}{1 + (1-\eta)\sigma}}. \tag{14}$$

3 THE TERMINATION SHOCK IN A STRIPED PULSAR WIND

In a striped wind, the magnetic field forms toroidal stripes of opposite polarity, separated by current sheets (Michel 1971, 1982; Bogovalov 1999). Such a structure arises in the equatorial belt of the pulsar wind and may be considered as an entropy wave propagating through the wind. Usov (1975) and Michel (1982) noticed that the waves must decay at large distances, since the current required to sustain them falls off as r^{-1}, whereas the density of available charge carriers in the wind decreases as r^{-2}. Hence the alternating magnetic fields should eventually annihilate. It was shown in LK that the distance beyond which the available charge carriers are unable to maintain the necessary current exceeds the radius of the standing shock where the wind terminates so that only some fraction of the magnetic energy is converted into particle energy before the plasma reaches this shock front. This fraction depends on the magnetic field reconnection rate. A lower limit may be obtained by assuming that the dissipation keeps the width of the current sheet equal to the particle Larmor radius, which is roughly the same condition as the current velocity being equal to the speed of light (Coroniti 1990; Michel 1994; LK). Then approximately 10 per cent of the Poynting flux dissipates before the wind reaches the termination shock. At a higher reconnection rate the fraction of the dissipated energy is larger; assuming that the reconnection velocity is as high as the sound velocity one can find that the alternating field annihilates completely before the flow enters the termination shock (Kirk & Skjæraasen 2003). Here I adopt the slow reconnection model by LK to estimate the flow parameters just upstream of the termination shock.

Neglecting the dependence of the wind parameters on latitude, one can express them only via the pulsar spin-down power, $L_{\rm sd}$, and the total number of the ejected electrons, $\dot{N}$. LK used instead the ratio of the gyro-frequency at the light cylinder to the angular velocity of the neutron star and the so-called multiplicity coefficient arising in the models of the pair production in pulsar magnetospheres. These parameters may be expressed via $L_{\rm sd}$ and $\dot{N}$ taking into account that the magnetic field at the light cylinder is estimated as $B_{\rm L} = \sqrt{L_{\rm sd}/(cR_{\rm l})}$, where $R_{\rm l} = cP/2\pi$ is the light cylinder radius and P is the pulsar period.

The characteristic distance beyond which the available charge carriers are unable to maintain the necessary current (equation 14 in LK) may be written as

$$R_{\max} = \frac{\pi}{2}\sqrt{\frac{e^2 L_{\rm sd}}{m_e^2 c^5}}R_{\rm l}, \tag{15}$$

where e is the electron charge. For the Crab Nebula $R_{\max} = 1.9 \times 10^{19}$ cm. Note that the dimensionless parameter $\hat{L}$ used by Kirk & Skjæraasen (2003) is proportional to $(R_{\max}/R_{\rm l})^2$. In the Poynting-dominated flows, dissipation of even a small fraction of the Poynting flux implies significant acceleration of the flow. While the dissipated energy is small, the Lorentz factor of the wind (equation 30 in LK) may be estimated as

$$\Gamma_{\rm w} = \frac{1}{2}\Gamma_{\max}\sqrt{\frac{R}{R_{\max}}}, \tag{16}$$

where

$$\Gamma_{\max} = \frac{L_{\rm sd}}{m_e c^2 \dot{N}} \tag{17}$$

is the Lorentz factor attained by the wind if all the spin-down power is converted into the kinetic energy of the plasma. Note that $\Gamma_{\rm w}/\Gamma_{\max}$ is the fraction of the spin-down power transferred to the plasma, therefore the magnetization parameter of the wind may be written as

$$\sigma = \frac{\Gamma_{\max}}{\Gamma_{\rm w}} - 1. \tag{18}$$

The current sheet width is conveniently measured by a fraction Δ of a wavelength $2\pi\ R_{\rm l}$ occupied by the two current sheets; equation (31) in LK may be written as

$$\Delta = \frac{1}{6}\sqrt{\frac{R}{R_{\max}}}. \tag{19}$$

In the Crab Nebula, the termination shock is observed at the distance 4×10^{17} cm (Weisskopf et al. 2000), therefore just upstream of the shock $\sigma = 13$, $\Delta = 0.024$, $\Gamma_{\rm w} = 4.4 \times 10^3/\dot{N}_{40}$, where $\dot{N}_{40} = \dot{N}/(10^{40}\ \mathrm{s}^{-1})$.

At the termination shock, the flow decelerates sharply so the plasma is compressed. The proper density grows Γ_1/Γ_2 times. According to equations (10) and (13), the smaller η (i.e. the larger the fraction of the magnetic flux dissipated at the shock) the smaller the downstream velocity is, so one can place a lower limit on the

compression factor assuming $\eta = 1$. In this case $\Gamma_2 = \sqrt{\sigma}$; substituting the estimated above parameters of the Crab wind, one obtains $\Gamma_1/\Gamma_2 = \Gamma_w/\sqrt{\sigma} \sim 1000$. Such a huge compression factor implies significant heating of the plasma, especially within the current sheets. Let us show that after such a compression the particle Larmor radius should exceed the wavelength so that the alternating magnetic field dissipates completely within the shock.

The downstream temperature, which determines the Larmor radius, depends on the fraction of the alternating magnetic field annihilated at the shock. Let us first assume that this fraction remains small so that the structure sketched in Fig. 1 is preserved downstream of the shock. The width of the current sheet in the wind frame cannot be less than the particle Larmor radius,

$$\delta = T/eB', \tag{20}$$

where T is the plasma temperature within the sheet and B' is the magnetic field in the wind frame of reference. The wavelength in the wind frame is $2\pi\ R_l\ \Gamma$, therefore the minimum fraction of the wavelength occupied by the two current sheets is

$$\Delta = T/(\pi R_l \Gamma e B').$$

The temperature obeys the condition of hydrostatic equilibrium of the plasma in the sheet, $n_h T = B'^2/8\pi$, where n_h is the number density of the plasma in the sheet. The magnetic field is frozen into the plasma outside the sheet, therefore $B' \propto n_c$, where n_c is the plasma number density outside the sheet. Now one can write (see equation 17 in LK)

$$\Delta \frac{n_h}{n_c} \propto \frac{1}{\Gamma}.$$

The left-hand side of this relation is the fraction of the particles carried in the sheet; of course this fraction should be less than unity. In the unshocked wind $n_h/n_c = 3$ (LK); with the above estimate for the upstream Δ, one obtains that upstream of the shock this fraction is approximately 0.1. It was demonstrated above that Γ decreases approximately 1000 times when the flow passes the shock, therefore downstream of the shock $\Delta\ n_h/n_c \sim 100$, which is impossible. This means that contrary to the initial assumption, the fraction of the magnetic field dissipated within the shock is not small and η defined by equation (4) is not close to unity.

In this case χ (equation 13) is also not close to unity and then, according to equations (10) and (12), the downstream flow is non- or mildly relativistic, $\Gamma_2 \sim 1$, whereas the downstream temperature is approximately the particle kinetic energy upstream of the shock, $T_2 \sim \Gamma_w \sigma m_e c^2$. With the above estimates for the upstream Lorentz factor and magnetization parameter, one can easily see that the Larmor radius downstream of the shock, $r_L = T/eB \sim 10^{12}/(B_{-4}\dot{N}_{40})$ cm, vastly exceeds the wavelength, $\lambda = 2\pi R_l = 10^9$ cm, therefore the alternating magnetic field should completely annihilate at the shock.

This means that the parameter χ should be determined as the ratio of the Poynting flux associated with the average magnetic field, $c\langle B\rangle^2/4\pi$, to the total energy flux. Therefore, the downstream parameters are independent of whether the alternating magnetic field dissipated upstream of the shock or just at the shock. The available upper limits on the magnetization parameter in the pulsar wind (Kennel & Coroniti 1984; Emmering & Chevalier 1987; Begelman & Li 1992) was found from the standard MHD shock conditions applied to the downstream parameters estimated from the analysis of the plasma dynamics in the nebula downstream of the shock. In the case of the striped wind these upper limits should be attributed not to the total Poynting flux but to the Poynting flux associated with the average magnetic field (see also Rees & Gunn 1974; Kundt & Krotscheck 1980). The upstream flow may be Poynting-dominated provided most of the electromagnetic energy is carried by the alternating magnetic field, which annihilates at the termination shock.

4 PARTICLE ACCELERATION BY DRIVEN RECONNECTION

The particle acceleration by driven reconnection may be described qualitatively as follows. Let us consider a box with two stripes of oppositely directed magnetic field and a current sheet between them (Fig. 2). When the box is compressed, an electric field $\boldsymbol{E} = -(1/c)\ \boldsymbol{v} \times \boldsymbol{B}$ arises, which has the same sign in the domains of opposite magnetic polarity. Close enough to the zero line of the magnetic field, particles may move freely along this line and gain energy from the electric field. Of course the real picture should be much more complicated than the one-dimensional sketch presented. The magnetic reconnection might proceed in separate X-points but on average the process remains one dimensional because the released energy is confined to a layer around the field reversal.

Acceleration of relativistic electrons close to an X-point was considered by Romanova & Lovelace (1992), Zenitani & Hoshino (2001) and Larrabee et al. (2003), who found a power-law particle distribution with a slope of $\beta \sim 1$. Reconnection in a long current sheet at a time-scale large enough that particles pass many X-points has not been considered yet. Let us assume that a power-law distribution is also formed in this case and estimate the maximal energy particles attain when the magnetic field annihilates completely.

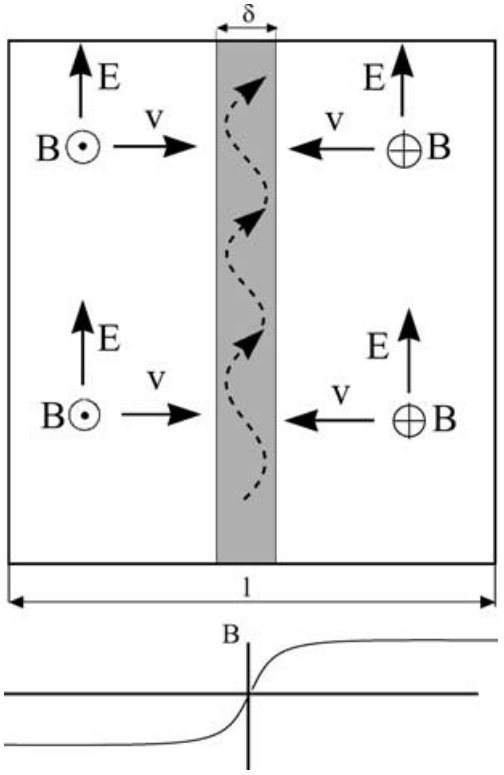

Figure 2. A compressing box with oppositely directed magnetic fields. The distribution of the magnetic field is shown at the bottom. The current sheet is shaded. The magnetic field is directed perpendicular to the plane of the figure. Directions of the velocities and the electric fields are shown by thick arrows. An unbounded particle trajectory near the field reversal is shown by dashed arrows.

Let the particle energy distribution within the current sheet be $N(\gamma) = K\gamma^{-\beta}$ at $1 \leqslant \gamma \leqslant \gamma_{\rm m}$ with $\beta \sim 1-2$. At such a distribution function, the particle density is dominated by low-energy electrons,

$$n_{\rm h} = \frac{K}{\beta - 1}, \tag{21}$$

whereas the energy density is dominated by high-energy electrons,

$$\varepsilon = \frac{m_{\rm e}c^2 K}{2-\beta}\gamma_{\rm m}^{2-\beta}. \tag{22}$$

Let us assume that the power-law index β remains fixed in the course of compression and only K and $\gamma_{\rm m}$ vary. One can find these variations by considering particle and energy balance within the box.

The particle balance is written as

$$n_{\rm h}\delta + n_{\rm c}(l-\delta) = n_{\rm h0}\delta_0 + n_{\rm c0}(l_0 - \delta_0), \tag{23}$$

where δ is the sheet width, l the box width, $n_{\rm h}$ and $n_{\rm c}$ are the particle number densities in the sheet and outside it, respectively, and the index 0 refers to the initial state. The energy balance implies that the variation of the total energy within the box is equal to the work performed on the box by the outer pressure ($=B^2/8\pi$):

$$\mathrm{d}\left[\varepsilon\delta + (l-\delta)\frac{B^2}{8\pi}\right] = -\frac{B^2}{8\pi}\,\mathrm{d}l,$$

where ε is the plasma energy density in the sheet. Taking into account that the magnetic field is frozen into the cold plasma,

$$B = bn_{\rm c}, \tag{24}$$

and that the plasma pressure in the sheet, $p = \varepsilon/3$, is counterbalanced by the magnetic pressure,

$$\frac{\varepsilon}{3} = \frac{B^2}{8\pi}, \tag{25}$$

one can write the energy balance equation in the form

$$(l+2\delta)\frac{\mathrm{d}n_{\rm c}}{\mathrm{d}l} + n_{\rm c}\frac{\mathrm{d}\delta}{\mathrm{d}l} + n_{\rm c} = 0. \tag{26}$$

Let us assume that the sheet width is equal to the maximal Larmor radius

$$\delta = \frac{m_{\rm e}c^2\gamma_{\rm m}}{eB}.$$

The maximal Lorentz factor, $\gamma_{\rm m}$, is found from equations (21), (22), (24) and (25) as

$$\gamma_{\rm m} = \left[\frac{3(2-\beta)}{8\pi(\beta-1)}\frac{b^2 n_{\rm c}^2}{m_{\rm e}c^2 n_{\rm h}}\right]^{1/(2-\beta)}. \tag{27}$$

Now one can write

$$\delta = \delta_0\left(\frac{n_{\rm c}}{n_{\rm c0}}\right)^{\beta/(2-\beta)}\left(\frac{n_{\rm h0}}{n_{\rm h}}\right)^{1/(2-\beta)}. \tag{28}$$

In order to find the plasma parameters in the course of compression one should solve equations (23), (26) and (28) for $\delta(l)$, $n_{\rm c}(l)$, $n_{\rm h}(l)$ from $l = l_0$ to smaller l. The magnetic field dissipates completely when the sheet width becomes comparable to the box width, $\delta \sim l$. At the final stage, one is unable to separate unambiguously the total plasma volume on to a hot current sheet and a cold magnetized plasma, therefore the presented equations may only be used to gain a rough estimate of the final plasma parameters. Taking this into account, one can simplify the problem even more and solve these equations in the limit $\delta \ll l$, when they are formally applicable, and take the limit $\delta = l$ in the obtained solutions.

Let us introduce the dimensionless variable $\Delta \equiv \delta/l$. In the zeroth order in small Δ, both equations (23) and (26) reduce to the same equation,

$$n_{\rm c}l = n_{\rm c0}l_0, \tag{29}$$

so the system is nearly degenerate. In order to find the second equation, one should expand equations (23) and (26) to the first order in Δ and eliminate the zeroth-order term. Introducing one more dimensionless variable $Y \equiv n_{\rm h}/n_{\rm c}$, one obtains

$$\Delta l\frac{\mathrm{d}Y}{\mathrm{d}l} + (Y-2)l\frac{\mathrm{d}\Delta}{\mathrm{d}l} + \Delta = 0. \tag{30}$$

Transforming equation (28) to the dimensionless variables Δ and Y and substituting $n_{\rm c}$ from equation (29), one obtains

$$\frac{\Delta}{\Delta_0} = \left(\frac{Y_0 l_0}{Yl}\right)^{1/(2-\beta)}. \tag{31}$$

Now one can eliminate l from equations (30) and (31) to finally obtain

$$(Y-1)\frac{\Delta}{Y}\frac{\mathrm{d}Y}{\mathrm{d}\Delta} + Y + \beta - 4 = 0. \tag{32}$$

The solution to this equation is

$$\left(\frac{\Delta}{\Delta_0}\right)^{4-\beta} = \frac{Y_0}{Y}\left(\frac{Y_0+\beta-4}{Y+\beta-4}\right)^{3-\beta}.$$

At $\Delta \gg \Delta_0$ (but still $\Delta \ll 1$) Y goes to a constant, $Y = 4-\beta$, independent of the initial conditions. Taking into account that in the pulsar wind $Y = 3$ (LK), one can take for estimates $Y = Y_0 = 3$.

Now one can estimate the compression factor, $k \equiv l_0/l$, necessary for the magnetic field to dissipate completely. Substituting $\Delta = 1$ into equation (31), one obtains

$$k = \Delta_0^{\beta-2}. \tag{33}$$

Substituting $n_{\rm c} = kn_{\rm c0}$ into equation (27) yields an estimate for the maximal Lorentz factor attained when the magnetic field dissipates completely,

$$\gamma_{\rm m} = \frac{1}{\Delta_0}\left[\frac{(2-\beta)}{2(\beta-1)}\sigma\right]^{1/(2-\beta)}, \tag{34}$$

where $\sigma = b^2 n_{\rm c0}/(4\pi m_{\rm e}c^2)$ is the initial magnetization parameter. It follows from equations (16), (18) and (19) that in the wind upstream of the shock $\Delta \sim 1/\sigma$, therefore the particles may be accelerated up to large energies, $\gamma_{\rm m} \gg 1$, even at a moderately large σ.

5 PARTICLE ACCELERATION AT THE TERMINATION SHOCK IN A STRIPED WIND

At the termination shock, the flow is compressed and the energy of the alternating magnetic field is released. Close to the equator of the flow, the average magnetic field is small and nearly all the Poynting flux is transferred to the particles. It was shown in Section 2 that the downstream velocity is non-relativistic in this case, therefore the proper density of the plasma increases by $\sim\Gamma_{\rm w}$ times, where $\Gamma_{\rm w}$ is the wind Lorentz factor upstream of the shock. For typical parameters (see Section 3) this compression factor significantly exceeds that given by equation (33); this confirms the conclusion that the alternating magnetic field annihilates completely at the termination shock.

The flow is decelerated in the shock by the pressure of the hot downstream plasma and magnetic field. In the collisionless shock the deceleration scale is approximately the Larmor radius of those particles that make a major contribution to the downstream pressure.

These particles penetrate upstream by their Larmour radius and exert, via the magnetic field, a decelerating force on the upstream flow. In the standard MHD shock, the downstream temperature is approximately the particle kinetic energy in the upstream flow, therefore the upstream particles penetrate approximately all the shock width immediately after they enter the shock. So there is only one characteristic spatial scale in this case, namely that of the Larmor radius corresponding to the upstream kinetic energy. In the shock in the striped wind, the particles gain energy from the annihilating magnetic field so that the downstream pressure is determined by particles with energy significantly exceeding the upstream kinetic energy. The Larmor radius of these particles significantly exceeds not only the Larmor radius corresponding to the kinetic energy in the upstream flow but even the strip width. Therefore, the width of such a shock, or the deceleration scale, exceeds all 'internal' scales in the upstream flow and hence the field annihilation proceeds locally in the proper frame such as in the plasma smoothly compressed by an external force. Only when the alternating field dissipates completely does the particle Larmor radius (calculated taking into account both thermal and kinetic energy) become comparable to the shock width and the flow decelerate further on as in the standard shock. So one can roughly separate the shock into two zones. In the first zone, the flow is decelerated and compressed by the pressure of high-energy particles entering from the second zone. The magnetic field dissipates in the first zone roughly according to the simple picture outlined in Section 4. The plasma heated by the field annihilation in the first zone enters the second one, therefore the second zone resembles the standard shock with a hot upstream plasma.

The compression factor, k, necessary for the magnetic field to dissipate completely was estimated in the previous section. The continuity equation in the relativistic flow, $n\Gamma = \text{constant}$, implies that the flow Lorentz factor at the end of the field dissipation stage is $\Gamma_{\rm d} \sim \Gamma_{\rm w}/k$. Adopting the picture of the particle acceleration by driven reconnection outlined in the previous section, one concludes that a power-law particle distribution is formed at this stage. In the proper plasma frame moving with the Lorentz factor $\Gamma_{\rm d}$, this distribution extends from $\gamma \sim 1$ up to $\gamma \sim \gamma_{\rm m}$. Now the alternating field is already dissipated and the flow decelerates further on, from $\Gamma \sim \Gamma_{\rm d}$ down to $\Gamma \sim 1$, such as in the standard MHD shock. Applying the particle and energy flux conservation, $n\Gamma\, v = \text{constant}$ and $\varepsilon\Gamma^2 v = \text{constant}$, one finds the maximal energy in the particle distribution downstream of the shock, $\gamma_{\rm max} \sim \Gamma_{\rm d}\gamma_{\rm m}$. The upper limit on the minimal energy may be estimated from the condition that the energy of most of the particles is simply randomized but does not change considerably; then $\gamma_{\rm min} \sim \Gamma_{\rm d}$. Making use of equations (33) and (34), one obtains

$$\gamma_{\rm min} \sim \Delta^{2-\beta}\Gamma_{\rm w}, \tag{35}$$

$$\gamma_{\rm max} \sim \frac{\Gamma_{\rm w}}{\Delta^{\beta-1}}\left[\frac{2-\beta}{2(\beta-1)}\sigma\right]^{1/(2-\beta)}. \tag{36}$$

Substituting $\beta = 1.5$ and parameters for the Crab pulsar wind upstream of the termination shock (see Section 3), one obtains $\gamma_{\rm min} \sim 600$, $\gamma_{\rm max} \sim 10^6$, which is roughly compatible with the parameters inferred from the observed spectrum.

These simple estimates show that particle acceleration at the shock in a striped wind may form such a particle distribution that the energy of most of the particles is significantly less than the upstream particle kinetic energy, whereas the plasma energy density is dominated by a relatively small number of high-energy particles. These high-energy particles may be accelerated further on by the first-order Fermi mechanism, thus forming a high-energy tail at $\gamma > \gamma_{\rm max}$. Recent investigations (Bednarz & Ostrowski 1998; Gallant & Achterberg 1999; Kirk et al. 2000; Achterberg et al. 2001) have shown that in ultrarelativistic shocks, the tail is formed with a power-law index $\beta = 2.2$–2.3, compatible with the observed X-ray spectra of the Crab Nebula and other plerions. So the observed broken power-law spectrum with a flat low-frequency part may be attributed to the particle acceleration at the termination shock in a striped pulsar wind.

6 CONCLUSIONS

The observed spectra of plerions from the radio to the gamma-ray band imply a very wide electron energy distribution, from less than a few hundred MeV to $\sim 10^{16}$ eV. Most of electrons are accumulated at the low-energy end of this distribution. Although the synchrotron lifetime of these electrons exceeds the plerion age, there is strong evidence to suggest that they are accelerated now together with high-energy electrons responsible for the hard radiation from the nebula (Bietenholtz & Kronberg 1992; Gallant & Tuffs 1999; Gallant & Tuffs 2002; Bietenholtz et al. 2001). The observed flat radio spectrum implies that the acceleration mechanism transfers most of the available energy to a small fraction of particles and retains most of particles at relatively low energy.

It is proposed in this article that the flat energy distribution is formed in the course of the particle acceleration by driven reconnection of the alternating magnetic field at the pulsar wind termination shock. It is widely believed that just upstream of the termination shock the magnetic energy is negligible compared with the plasma kinetic energy because plasma dynamics in the nebula implies small magnetization downstream of the shock (Rees & Gunn 1974; Kennel & Coroniti 1984; Emmering & Chevalier 1987; Begelman & Li 1992). However, the plasma magnetization and dynamics depend only on the average upstream magnetic field so the upstream flow may be Poynting-dominated provided most of the magnetic energy is associated with the alternating magnetic field. In this case the average particle energy grows significantly at the shock where the magnetic field annihilates. Therefore, a particle distribution with power-law index $\beta < 2$ is formed readily.

The proposed mechanism may also explain why no low-frequency cut-off is observed in the Crab radio spectrum. At the kinetic-energy-dominated shocks, the power-law tail is formed only at energies exceeding the downstream temperature, which is approximately the particle kinetic energy upstream of the shock. Therefore, if the Crab pulsar wind were kinetic-energy-dominated, only a rather low Lorentz factor for the wind would be compatible with the radio data, which would imply an extremely highly mass loaded wind. In the striped wind, most of the energy is contained in the magnetic field, therefore the wind Lorentz factor is lower than in the kinetic-energy-dominated wind. Moreover, the simple model of the shock in a striped wind presented here predicts that in this case the downstream temperature may be considerably less than the upstream particle kinetic energy. Therefore, the lack of a low-frequency turnover in the observed plerion spectra may be naturally explained within the scope of the proposed model. Of course the qualitative picture of the particle acceleration in plerions outlined here may be considered only as preliminary; it may be justified only by numerical simulations of the shock in a striped wind.

ACKNOWLEDGMENT

I am grateful to David Eichler for stimulating discussions.

REFERENCES

Achterberg A., Gallant Y.A., Kirk J.G., Guthmann A.W., 2001, MNRAS, 328, 393
Appl S., Camenzind M., 1988, A&A, 206, 258
Arons J., 1983, in Burns M.L., Harding A.K., Ramaty R., eds, Positron–Electron Pairs in Astrophysics. AIP, New York, p. 163
Atoyan A.M., 1999, A&A, 346, L49
Bednarz J., Ostrowski M., 1998, Phys. Rev. Lett., 80, 3911
Begelman M.C., Li Z.-Y., 1992, ApJ, 397, 187
Bietenholtz M.F., Kronberg P.P., 1992, ApJ, 393, 206
Bietenholtz M.F., Frail D.A., Hester J.J., 2001, ApJ, 560, 254
Birk G.T., Crusius-Wätzel A.R., Lesch H., 2001, ApJ, 559, 96
Bogovalov S.V., 1999, A&A, 349, 101
Cheng A.F., Ruderman M.A., 1980, ApJ, 235, 576
Coroniti F.V., 1990, ApJ, 349, 538
Emmering R.T., Chevalier R.A., 1987, ApJ, 321, 334
Gaensler B.M., Pivovaroff M.J., Garmire G.P., 2001, ApJ, 556, L107
Gaensler B.M., Arons J., Kaspi V.M., Pivovaroff M.J., Kawai N., Tamura K., 2002, ApJ, 569, 878
Gallant Y.A., Achterberg A., 1999, MNRAS, 305, L6
Gallant Y.A., Arons J., 1994, ApJ, 435, 230
Gallant Y.A., Tuffs R.J., 1999, in Kramer M., Wex N., Wielebinski N., eds, ASP Conf. Ser., Vol. 202; Proc. IAU Coll. 177, Pulsar Astronomy – 2000 and Beyond. Astron. Soc. Pac., San Francisco, p. 503
Gallant Y.A., Tuffs R.J., 2002, in Slane P.O., Gaensler B.M., eds, ASP Conf. Ser., Vol. 271, Neutron Stars in Supernova Remnants. Astron. Soc. Pac., San Francisco, p. 161
Gallant Y.A., van der Swaluw E., Kirk J.G., Achterberg A., 2002, in Slane P.O., Gaensler B.M., eds, ASP Conf. Ser., Vol. 271, Neutron Stars in Supernova Remnants. Astron. Soc. Pac., San Francisco, p. 99
Helfand D.J., Gotthelf E.V., Halpern J.P., 2001, ApJ, 556, 380
Hoshino M., Arons J., Gallant Y.A., Langdon A.B., 1992, ApJ, 390, 454
Kennel C.F., Coroniti F.V., 1984, ApJ, 283, 694
Kirk J.G., Skjæraasen O., 2003, ApJ, 591, 366
Kirk J.G., Guthman A.W., Gallant Y.A., Achterberg A., 2000, ApJ, 542, 235
Kundt W., Krotscheck E., 1980, A&A, 83, 1
Larrabee D.A., Lovelace R.V.E., Romanova M.M., 2003, ApJ, 586, 72
Levinson A., van Putten P.M., 1997, ApJ, 488, 69
Lu F.J., Wang Q.D., Aschenbach B., Durouchoux P., Song L.M., 2002, ApJ, 568, L49
Lyubarsky Y.E., Kirk J.G., 2001, ApJ, 547, 437 (LK)
Lyutikov M., 2002, preprint (astro-ph/0210353)
Michel F.C., 1971, Comments Astrophys. Space Phys., 3, 80
Michel F.C., 1982, Rev. Mod. Phys., 54, 1
Michel F.C., 1994, ApJ, 431, 397
Pavlov G.G., Kargaltsev O.Y., Sanwal D., Garmire G.P., 2001, ApJ, 554, L189
Rees M.J., Gunn J.E., 1974, MNRAS, 167, 1
Romanova M.M., Lovelace R.V.E., 1992, A&A, 262, 26
Shklovsky I.S., 1970, ApJ, 159, L77
Usov V.V., 1975, ApSS, 32, 375
Weisskopf C. et al., 2000, ApJ, 536, L81
Zenitani S., Hoshino M., 2001, ApJ, 562, L63

This paper has been typeset from a TEX/LATEX file prepared by the author.